Fluorescence Probes

International Edition: DOI: 10.1002/anie.201500537
German Edition: DOI: 10.1002/ange.201500537

Development of Imidazoline-2-Thiones Based Two-Photon Fluorescence Probes for Imaging Hypochlorite Generation in a Co-Culture System**

Qingling Xu, Cheol Ho Heo, Gyoungmi Kim, Hyo Won Lee, Hwan Myung Kim, and Juyoung Yoon**

Abstract: *We designed and prepared the imidazoline-2-thione containing OCl^- probes,* ***PIS*** *and* ***NIS****, which operate through specific reactions with OCl^- that yield corresponding fluorescent imidazolium ions. Importantly, we demonstrated that* ***PIS*** *can be employed to image OCl^- generation in macrophages in a co-culture system. We have also employed two-photon microscopy and* ***PIS*** *to image OCl^- in live cells and tissues, indicating that this probe could have wide biological applications.*

Reactive oxygen species (ROS) are important and prevalent mediators of many biological processes.[1,2] The brain is particularly sensitive to ROS-induced oxidative stress, which results from an imbalance between the aberrant formation of ROS and defense against these substances provided by antioxidants.[3–5] Hypochlorite (OCl^-), a prominent member of ROS,[6,7] is mainly produced by the myeloperoxidase (MPO) catalyzed reaction of H_2O_2 and Cl^- in immunocytes.[8] OCl^- plays an important role in controlling invading microbes.[9–11] On the other hand, OCl^- reacts rapidly with a variety of biomolecules[12,13] and is connected with various disorders.[14] To understand the physiological and pathological roles of OCl^-, it is crucial to be able to monitor and image the location of OCl^- at the cell, tissue, and organism levels.

Small molecule fluorescent probes serve as superior tools in imaging studies.[15] Fluorescent probes for detecting H_2O_2,[16] NO,[17] $ONOO^-$,[18] $^1O_2$,[19] $\cdot O_2^-$[20], and OCl^-[21] have recently been developed. However, these probes have limitations imposed by short excitation wavelengths in the UV to visible range, which result in shallow tissue penetration depths, autofluorescence, and artificial ROS generation.[22]

Two-photon microscopy (TPM) is an attractive approach for detecting OCl^- in live cells and tissues.[23–25] In contrast to one-photon microscopy, TPM has many advantageous features such as greater tissue penetration depths ($>500\ \mu m$), higher spatial resolution, and lower phototoxicity.[26–28] However, to the best of our knowledge, no report exists describing a TPM-based probe for direct imaging of endogenous OCl^- produced in both live cells and tissues.

A fundamentally important yet challenging feature of studies in this area is the design of new chemorecognition processes. Imidazolium salts with good water solubility and stability, have been utilized as fluorescence sensors in aqueous solution.[29,30] Taking advantages of imidazolium salts, we designed imidazoline-2-thiones, **PIS** and **NIS**, as fluorescent OCl^- probes. The probes display highly selective and sensitive fluorescence turn-on responses to OCl^- and they can be utilized to image OCl^- generation in macrophages co-cultured with HeLa cells. More importantly, **PIS** can be combined with TPM to image OCl^- in cells and tissues.

The preparation of **PIS** and **NIS** is shown in Scheme 1. One sequence begins with reaction of the fused imidazole **1** and CH_3I to form the *N*-methyl derivative **2** (55%), which is then subjected to reaction with CH_3I under reflux conditions to generate the imidazolium salt **3** (29%). Treatment of **3** with sulfur leads to the formation of **PIS** (62%). In the other route,

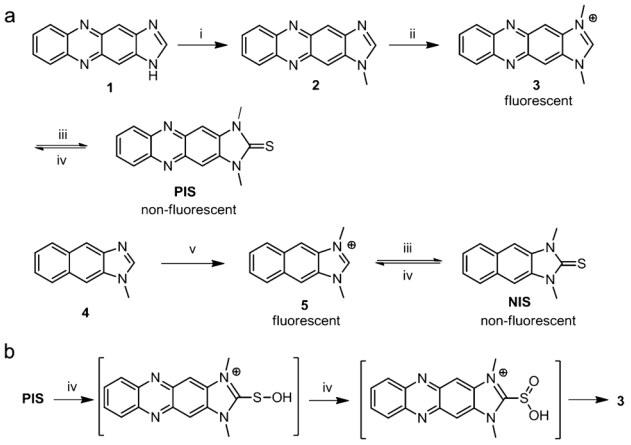

Scheme 1. a) Synthesis of imidazoline-2-thiones and b) the proposed reaction mechanism with OCl^-. Reagents and conditions: i) CH_3I, NaH/THF, RT; ii) CH_3I, reflux; iii) potassium *tert*-butoxide, sulfur/CH_3OH, 65 °C; iv) NaOCl; v) CH_3I/CH_3CN, reflux.

[*] Dr. Q. Xu,[+] G. Kim, Prof. J. Yoon
Department of Chemistry and Nano Science
Ewha Womans University
Seoul 120-750 (Korea)
E-mail: jyoon@ewha.ac.kr
C. H. Heo,[+] H. W. Lee, Prof. H. M. Kim
Department of Energy Systems Research, Ajou University
Suwon, Gyeonggi-do 443-749 (Korea)
E-mail: kimhm@ajou.ac.kr
[+] These authors contributed equally to this work.

[**] J.Y. acknowledges a grant from the National Creative Research Initiative programs of the National Research Foundation of Korea (NRF) funded by the Korean government (MSIP; 2012R1A3A2048814). H.M.K. acknowledges a grant from the National Research Foundation of Korea (NRF) funded by the Korean government (MSIP; 2012R1A2A1A03670456).
Supporting information for this article is available on the WWW under http://dx.doi.org/10.1002/anie.201500537.

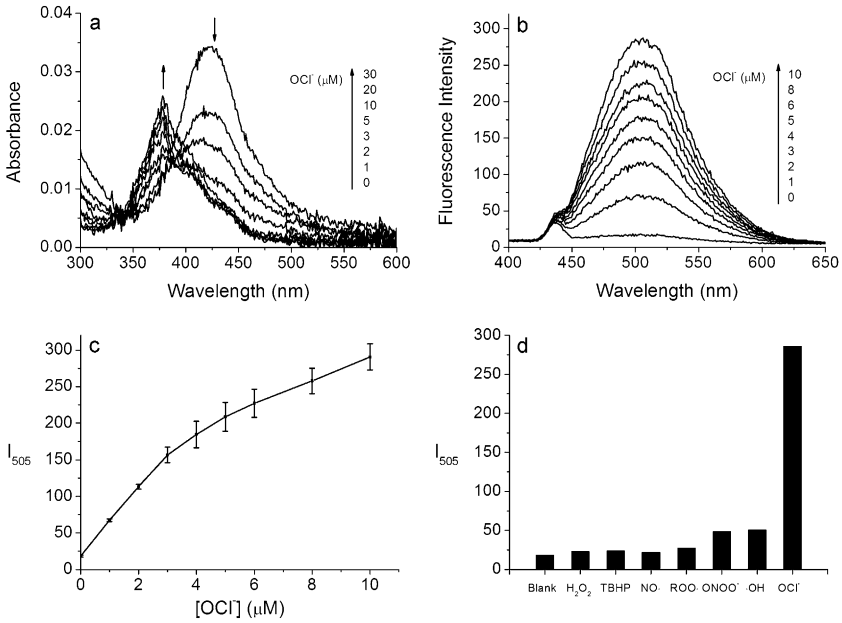

Figure 1. a) UV/Vis and b) fluorescence spectra changes of **PIS** solution during the titration of OCl^-. c) Fluorescence intensity at 505 nm of **PIS** solution with titration of OCl^- and d) fluorescence intensity at 505 nm of **PIS** solution over various ROS: OCl^- (10 μM), ROO· (1 mM), NO· (1 mM), H_2O_2 (1 mM), TBHP (1 mM), $ONOO^-$ (100 μM), ·OH (200 μM). [**PIS**] = 2 μM, in PBS buffer (50 mM, pH 7.4), excitation wavelength: 378 nm (slit widths: 5 nm/10 nm). $\rho_{DMF} = 0.1\%$.

reaction of naphthoimidazole **4** with CH_3I gives the imidazolium salt **5** (89%), which is then converted to **NIS** by treatment with sulfur (93%). The stock solutions of **PIS** and **NIS** were prepared using DMF as solvents.

The spectroscopic responses of the probes to ROS were monitored by UV/Vis absorption and fluorescence emission spectroscopy. Analysis of the spectra displayed in Figure 1a shows that the absorbance peak for **PIS**, centered at ca. 420 nm, dramatically decreases and a new peak at ca. 378 nm appears upon addition of up to 5 μM OCl^-. The new peak at 378 nm matches that of **3** (Figure S1). In addition, in PBS (pH 7.4) **PIS** has a low fluorescence efficiency (Figure 1b and c, Table S1). Addition of OCl^- to give final concentrations of 0–10 μM causes a rapid rise in a new emission band centered at around 505 nm. The fluorescence intensity was stable over a period of 2.5 h (Figure S2). The detection limit of **PIS** for OCl^- was determined to be 0.071 μM. Importantly other ROS including H_2O_2, NO·, ROO·, $ONOO^-$, ·OH, and *tert*-butyl hyperoxide (TBHP) even at higher concentrations and after incubation for 30 min, do not induce obvious fluorescence changes of **PIS** solutions (Figure 1d). The UV/Vis and fluorescence spectral changes of **NIS** brought about by OCl^- were also probed (Figure S3). The absorbance peak of **NIS** at 342 nm was found to decrease and a peak at ca. 325 nm appears upon addition of OCl^-. The fluorescence intensity of **NIS** solution increases significantly upon addition of OCl^-. Finally, ^1H NMR monitoring of preparative reactions of **PIS** and **NIS** with OCl^- shows that the processes generate imidazolium salts **3** and **5,** respectively (Figures S4 and S5); the proposed reaction mechanism is shown in Scheme 1b. The above results suggest that reactions of the probes with OCl^- occur both rapidly and efficiently to form the corresponding highly fluorescent imidazolium salts. As OCl^- generation in macrophages happens under acidic environment, we also studied the performance of **PIS** in acidic solution (50 mM KH_2PO_4, pH 5.0). The results show that **PIS** has a turn-on fluorescence response and high selectivity to OCl^- over other ROS (Figure S6).

To demonstrate the potential bioapplications of these probes, the ability of **PIS** to track intracellular OCl^- was determined. We firstly examined the cytotoxicity with HeLa cells and RAW 264.7 macrophages. The results show that the viability of HeLa cells is 95.7% when they are incubated with 10 μM **PIS** for 6 h (Figure S7), and the viability of macrophages is 93% after 2 h incubation with 100 μM **PIS**, indicating that **PIS** has low cytotoxicity. Then HeLa cells were treated with NaOCl (100 μM and 200 μM), followed by incubation with **PIS**, and fluorescence images of the cells were acquired. Inspection of the images displayed in Figure S8 shows that green fluorescence arises from cells that are treated with OCl^-, whereas cells incubated only with **PIS** do not fluoresce. Although HeLa cells were reported to produce OCl^- (8.23 nM),[21f] we think the concentration is too low to be imaged sufficiently by **PIS**. These observations show that **PIS** penetrates into the living cells, in which it produces a turn-on fluorescence response to OCl^-.

We chose RAW 264.7 macrophages to use **PIS** for the visualization of OCl^- generation. RAW 264.7 macrophages were activated by incubation with lipopolysaccharides (LPS) and then IFN-γ.[31] Phorbol myristate acetate (PMA) were used to produce H_2O_2, which is then transformed to OCl^- by MPO. Then RAW 264.7 macrophages were treated with **PIS** before being subjected to fluorescence microscope analysis. As the images in Figure 2b reveal, bright green fluorescence occurs from RAW 264.7 macrophages, while no emission is observed from cells that are not subjected to the OCl^- producing conditions outlined above (Figure 2a). Additional evidence to support the imaging results described above was gained in studies using the known MPO inhibitors, 4-aminobenzoicacid hydrazide (ABAH) and flufenamic acid (FFA).[32] RAW 264.7 macrophages, which are treated with the two inhibitors along with PMA and then **PIS** under otherwise identical conditions, display highly attenuated fluorescence intensities (Figure 2c and d). The results demonstrate that **PIS** can be employed to visualize OCl^- production in macrophages.

Macrophages in tumor tissue, referred to as tumor-associated macrophages (TAMs), have been found to have pro-tumorigenic and antitumor activity.[33] As a result, the ability to image macrophages in tumor tissue should enable clarification of the interaction network connecting cancer

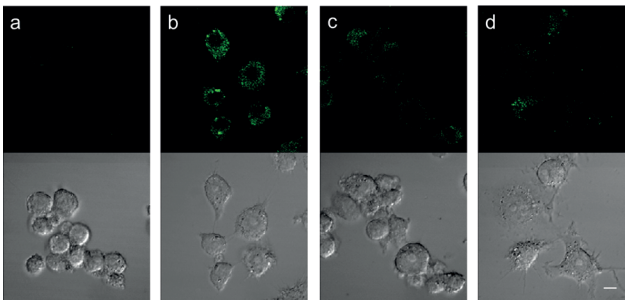

Figure 2. Fluorescence (upper) and differential interference contrast (DIC; lower) images of RAW 264.7 macrophages treated with various stimulants and then **PIS** (10 μM, $\rho_{DMF}=0.5\,\%$) for 20 min. a) **PIS**; b) LPS (100 ng mL^{-1}) for 16 h, IFN-γ (50 ng mL^{-1}) for 4 h, PMA (10 nM) for 30 min, and then **PIS**; c) LPS, IFN-γ, PMA + 4-ABAH (50 μM) for 16 h, and **PIS**; and d) LPS, IFN-γ, PMA + FFA (50 μM) for 16 h, and **PIS**. Scale bar: 10 μm.

cells and TAMs. To explore this feature, we designed a co-culture system to serve as a platform for imaging macrophages through **PIS**-promoted detection of produced OCl^-. For this purpose, RAW 264.7 macrophages were cultured together with HeLa cell, and then the cell mixtures were incubated with stimulants to generate OCl^-, and then with **PIS**. Inspection of the resulting fluorescence images displayed in Figure 3b shows that the macrophage and HeLa cell types have distinguishably different shapes. In addition, clear green fluorescence is emitted from the small round cells (blue arrow) that correspond to RAW 264.7 macrophages, whereas the large spindle cells (red arrow) corresponding to HeLa cells show negligible fluorescence. When the inhibitors ABAH and FFA are added along with PMA to the mixture of HeLa cells and RAW 264.7 macrophages, fluorescence emanating from the latter is greatly attenuated (Figure 3c and d). We also quantified and compared the fluorescence intensity from RAW 264.7 macrophages and HeLa cells using super-resolution microscopy. The results show that after treatment of stimulants, the fluorescence intensity from RAW 264.7 macrophages is 3.7-fold of that from HeLa cells (Figure S9). The results demonstrate conclusively that **PIS** can be employed to detect endogenous OCl^- produced in macrophages.

In the final phase of this study, we explored the utility of **PIS** to detect OCl^- by using TPM. The TP-excited fluorescence (TPEF) spectrum of **PIS** measured in RAW 264.7 cells has an emission maximum at 480 nm (Figure S10a), which is slightly blue-shifted from that measured in PBS buffer and nearly identical to those measured in EtOH (479 nm, Figure S1 and Table S1). This result suggests that EtOH can adequately represent the cellular environment of the probe. The TP action cross-section values ($\Phi\delta_{max}$, in which Φ is the fluorescence quantum yield and δ is the TP absorption cross section) of **PIS** and **3** in EtOH were determined to be 0.4 and 8.4 GM at 800 nm, whereas the δ_{max} values were 42 and 30 GM, respectively (Figure S10b and Table S1). The higher $\Phi\delta_{max}$ value of **3** is due to the higher Φ value (0.010 for **PIS** versus 0.28 for **3**). This predicts a significant TP turn-on response of the probe upon OCl^--induced **3** formation, as was observed (see below). Upon excitation at 800 nm with femtosecond (fs) pulses, the RAW 264.7 cells labeled with **PIS** display a dim TPEF (Figure 4a). When the cells are pretreated with OCl^-, the TPEF intensity is increased by more than 3-fold (Figure 4b and g). Similar observations were

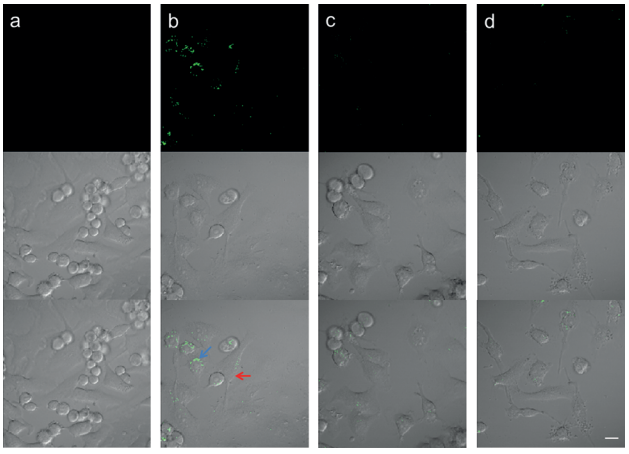

Figure 3. Fluorescence (upper) and bright-field (middle) and merge (lower) images of RAW 264.7 macrophages and HeLa cells treated with various stimulants and then incubated with **PIS** (10 μM, $\rho_{DMF}=0.5\,\%$) for 20 min. a) **PIS**; b) LPS (100 ng mL^{-1}) for 16 h, IFN-γ (50 ng mL^{-1}) for 4 h, PMA (10 nM) for 30 min, and then **PIS**; c) LPS, IFN-γ, PMA + 4-ABAH (50 μM) for 16 h, and **PIS**, and d) LPS, IFN-γ for 4 h, PMA + FFA (50 μM) for 16 h, and **PIS**. Scale bar: 10 μm. RAW 264.7 macrophages: small round cells (blue arrow), HeLa cells: large spindle cells (red arrow).

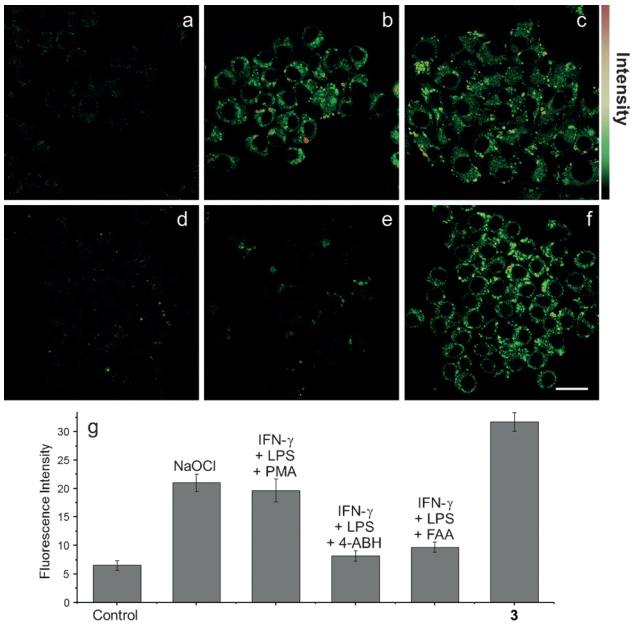

Figure 4. TPM images of RAW 264.7 cells labeled with a–e) **PIS** and f) **3** (10 μM, $\rho_{DMF}=0.5\,\%$). a) Control image. b) Cells pretreated with NaOCl (200 μM) for 30 min and then incubated with **PIS**. c) Cells pretreated with LPS (100 ng mL^{-1}) for 16 h, IFN-γ (400 U mL^{-1}) for 4 h, PMA (10 nM) for 30 min, and then **PIS**. d) Cells pretreated with LPS, IFN-γ, and 4-ABAH (50 μM) for 4 h, and then incubated with **PIS**. e) Cells pretreated with LPS, IFN-γ, and FAA (50 μM) for 4 h and then **PIS**. g) Average TPEF intensities in (a–f), $n=5$. Scale bar: 20 μm.

made in the TPM analysis after addition of the stimulants (100 ng mL^{-1} LPS, 400 U mL^{-1} IFN-γ) followed by 10 nM PMA (Figure 4c and g). Furthermore, the increase in emission intensity is suppressed when the MPO inhibitors, 4-ABAH and FAA (Figure 4d, e, and g), are present. These average intensities are between those measured in **PIS** and **3**-labeled cells (Figure 4f and g), confirming that the fluorescence signals in the TPM images directly reflect the presence of OCl$^-$. Moreover, the TPEF intensities of **PIS**-treated cells remain nearly the same after continuous irradiation with fs pulses for 60 min, even when the cells are pretreated with OCl$^-$. This observation demonstrates the high photostability and staining ability of **PIS** (Figure S11).

Finally, an investigation was conducted to evaluate the usefulness of **PIS** in monitoring OCl$^-$ in a fresh rat hippocampal slice. The TPM images of a slice that had been incubated with **PIS** and **3** display weak and strong fluorescence, respectively, in the CA1 and CA3 regions (Figure 5a, d and c, f). When tissue slices were first treated with different amounts of OCl$^-$, the TPEF intensities in both the CA1 and CA3 regions increase in a dose-dependent manner (Figure S12). In addition, the TPEF intensity increased when the tissue was stimulated with PMA (10 ng mL^{-1}; Figure 5b, e and h).[34] Moreover, the intense TPEF in PMA-treated tissue was mainly from microglia, rat hippocampus resident macrophages, as evidenced by immunostaining tests using the microglia-selective Iba1 antibody (Figure S13).[35] Moreover, the TPM images show that OCl$^-$ can be observed in the individual cells at a depth of more than 100 μm. These results conclusively demonstrate the capability of **PIS** to monitor OCl$^-$ in live tissues through the use of TPM.

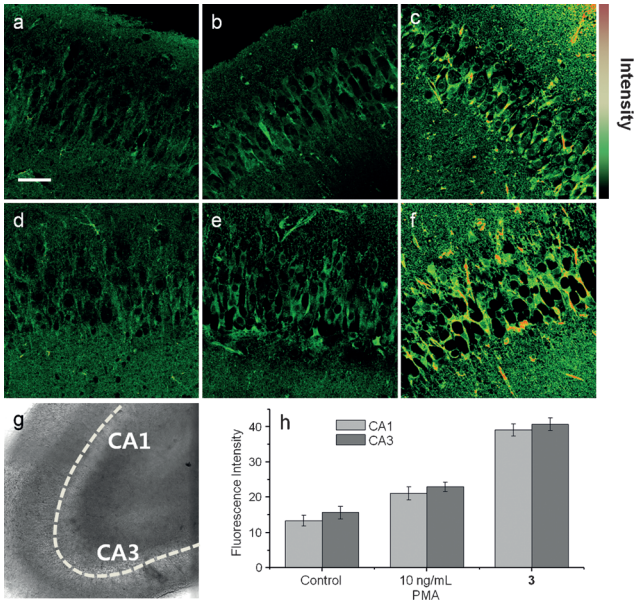

Figure 5. Images of a rat hippocampal slice stained with **PIS** and **3** (100 μM, ρ_{DMF} = 2.2%). a–f) TPM images of a rat hippocampal slice stained with a, d) 100 μM **PIS** and c, f) 100 μM **3** for 1.5 h, and b, e) pretreated with 10 ng mL^{-1} PMA for 30 min before labeling with 100 μM **PIS**. TPM images were taken at 40× magnification in the neuron layer of the a–c) CA1 and d–f) CA3 regions. g) Bright-field image of the CA1 and CA3 regions at 10× magnification. h) Average TPEF intensities in (a–f), n = 5. Scale bar: 48 μm.

In summary, we developed new, late-mode, turn-on fluorescent, imidazoline-2-thione probes for OCl$^-$ detection. One of these probes, **PIS**, was employed to image generated OCl$^-$ macrophages in a co-culture system. We also utilized a combination of this probe and TPM to image OCl$^-$ in cells and tissue.

Keywords: co-culture systems · fluorescence probes · hypochlorite generation · two-photon microscopy

How to cite: *Angew. Chem. Int. Ed.* **2015**, *54*, 4890–4894
Angew. Chem. **2015**, *127*, 4972–4976

[1] J. D. Lambeth, *Free Radicals Biol. Med.* **2007**, *43*, 332–347.
[2] S. G. Rhee, *Science* **2006**, *312*, 1882–1883.
[3] J. K. Andersen, *Nat. Rev. Neurosci.* **2004**, *5*, S18–S25.
[4] I. Silver, M. Erecinska, *Adv. Exp. Med. Biol.* **1998**, *454*, 7–16.
[5] R. A. Roberts, D. L. Laskin, C. V. Smith, F. M. Robertson, E. M. Allen, J. A. Doorn, W. Slikker, *Toxicol. Sci.* **2009**, *112*, 4–16.
[6] H. Wiseman, B. Halliwell, *Biochem. J.* **1996**, *313*, 17–29.
[7] N. Zhang, K. P. Francis, A. Prakash, D. Ansaldi, *Nat. Med.* **2013**, *19*, 500–505.
[8] N. M. Domigan, T. S. Charlton, M. W. Duncan, C. C. Winterbourn, A. J. J. Kettle, *Biol. Chem.* **1995**, *270*, 16542–16548.
[9] S. L. Hazen, F. F. Hsu, K. Duffin, J. W. Heinecke, *J. Biol. Chem.* **1996**, *271*, 23080–23088.
[10] K. M. Wynalda, R. C. Murphy, *Chem. Res. Toxicol.* **2010**, *23*, 108–117.
[11] S. Hammerschmidt, H. Wahn, *Am. J. Respir. Crit. Care Med.* **1997**, *156*, 924–931.
[12] A. Krasowska, G. W. Konat, *Brain Res.* **2004**, *997*, 176–184.
[13] C. C. Winterbourn, M. C. Vissers, A. J. Kettle, *Curr. Opin. Hematol.* **2000**, *7*, 53–58.
[14] T. M. Jeitner, H. Xu, G. E. Gibson, *J. Neurochem.* **2005**, *92*, 302–310.
[15] J. Chan, S. C. Dodani, C. J. Chang, *Nat. Chem.* **2012**, *4*, 973–984.
[16] a) N. Karton-Lifshin, E. Segal, L. Omer, M. Portnoy, R. Satchi-Fainaro, D. Shabat, *J. Am. Chem. Soc.* **2011**, *133*, 10960–10965; b) M. Abo, Y. Urano, K. Hanaoka, T. Terai, T. Komatsu, T. Nagano, *J. Am. Chem. Soc.* **2011**, *133*, 10629–10637; c) C. Chung, D. Srikun, C. S. Lim, C. J. Chang, B. R. Cho, *Chem. Commun.* **2011**, *47*, 9618–9620; d) G. Masanta, C. H. Heo, C. S. Lim, S. K. Bae, B. R. Cho, H. M. Kim, *Chem. Commun.* **2012**, *48*, 3518–3520; e) F. He, F. Feng, S. Wang, Y. Li, D. Zhu, *J. Mater. Chem.* **2007**, *17*, 3702–3707; f) D. B. M. Groegel, M. Link, A. Duerkop, O. S. Wolfbeis, *ChemBioChem* **2011**, *12*, 2779–2785; g) M. Kim, S. K. Ko, H. Kim, I. Shin, J. Tae, *Chem. Commun.* **2013**, *49*, 7959–7961; h) O. Redy-Keisar, E. Kisin-Finfer, S. Ferber, R. Satchi-Fainaro, D. Shabat, *Nat. Protoc.* **2014**, *9*, 27–36.
[17] a) A. T. Wrobel, T. C. Johnstone, A. D. Liang, S. J. Lippard, P. Rivera-Fuentes, *J. Am. Chem. Soc.* **2014**, *136*, 4697–4705; b) C. Sun, W. Shi, Y. Song, W. Chen, H. Ma, *Chem. Commun.* **2011**, *47*, 8638–8640; c) E. W. Miller, C. J. Chang, *Curr. Opin. Chem. Biol.* **2007**, *11*, 620–625; d) Y. Yang, S. K. Seidlits, M. M. Adams, V. M. Lynch, C. E. Schmidt, E. V. Anslyn, J. B. Shear, *J. Am. Chem. Soc.* **2010**, *132*, 13114–13116.
[18] a) X. Sun, Q. Xu, G. Kim, S. E. Flower, J. P. Lowe, J. Yoon, J. S. Fossey, X. Qian, S. D. Bull, T. D. James, *Chem. Sci.* **2014**, *5*, 3368–3373; b) X. Chen, T. Pradhan, F. Wang, J. S. Kim, J. Yoon, *Chem. Rev.* **2012**, *112*, 1910–1956.
[19] a) B. Song, G. Wang, M. Tan, J. Yuan, *J. Am. Chem. Soc.* **2006**, *128*, 13442–13450; b) K. Naito, T. Tachikawa, S. C. Cui, A.

Sugimoto, M. Fujitsuka, T. Majima, *J. Am. Chem. Soc.* **2006**, *128*, 16430 – 16431; c) K. Tanaka, T. Miura, N. Umezawa, Y. Urano, K. Kikuchi, T. Higuchi, T. Nagano, *J. Am. Chem. Soc.* **2001**, *123*, 2530 – 2536; d) S. Ozlem, E. U. Akkaya, *J. Am. Chem. Soc.* **2009**, *131*, 48 – 49; e) Y. Cakmak, S. Kolemen, S. Duman, Y. Dede, Y. Dolen, B. Kilic, Z. Kostereli, L. T. Yildirim, A. L. Dogan, D. Guc, E. U. Akkaya, *Angew. Chem. Int. Ed.* **2011**, *50*, 11937 – 11941; *Angew. Chem.* **2011**, *123*, 12143 – 12147.

[20] a) K. Kundu, S. F. Knight, N. Willett, S. Lee, W. R. Taylor, N. Murthy, *Angew. Chem. Int. Ed.* **2009**, *48*, 299 – 303; *Angew. Chem.* **2009**, *121*, 305 – 309; b) W. Zhang, P. Li, F. Yang, X. Hu, C. Sun, W. Zhang, D. Chen, B. Tang, *J. Am. Chem. Soc.* **2013**, *135*, 14956 – 14959; c) H. Maeda, K. Yamamoto, Y. Nomura, I. Kohno, L. Hafsi, N. Ueda, S. Yoshida, M. Fukuda, Y. Fukuyasu, Y. Yamauchi, N. Itoh, *J. Am. Chem. Soc.* **2005**, *127*, 68 – 69; d) M. Sekiya, K. Umezawa, A. Sato, D. Citterio, K. Suzuki, *Chem. Commun.* **2009**, 3047 – 3049.

[21] a) L. Yuan, W. Lin, H. Chen, *Biomaterials* **2013**, *34*, 9566 – 9571; b) Q. A. Best, N. Sattenapally, D. J. Dyer, C. N. Scott, M. E. McCarroll, *J. Am. Chem. Soc.* **2013**, *135*, 13365 – 13370; c) Y. Koide, Y. Urano, K. Hanaoka, T. Terai, T. Nagano, *J. Am. Chem. Soc.* **2011**, *133*, 5680 – 5682; d) Z. Lou, P. Li, Q. Pan, K. Han, *Chem. Commun.* **2013**, *49*, 2445 – 2447; e) J. J. Hu, N. K. Wong, Q. Gu, X. Bai, S. Ye, D. Yang, *Org. Lett.* **2014**, *16*, 3544 – 3547; f) H. Zhu, J. Fan, J. Wang, H. Mu, X. Peng, *J. Am. Chem. Soc.* **2014**, *136*, 12820 – 12823.

[22] M. J. Jou, S. B. Jou, M. J. Guo, H. Y. Wu, T. I. Peng, *Ann. N. Y. Acad. Sci.* **2004**, *1011*, 45 – 46.

[23] W. R. Zipfel, R. M. Williams, W. W. Webb, *Nat. Biotechnol.* **2003**, *21*, 1369 – 1377.

[24] F. Helmchen, W. Denk, *Nat. Methods* **2005**, *2*, 932 – 940.

[25] a) L. Li, X. Shen, Q. Xu, S. Q. Yao, *Angew. Chem. Int. Ed.* **2013**, *52*, 424 – 428; *Angew. Chem.* **2013**, *125*, 442 – 446; b) A. S. Rao, D. Kim, T. Wang, K. H. Kim, S. Hwang, K. H. Ahn, *Org. Lett.* **2012**, *14*, 2598 – 2601; c) H. Ahn, K. E. Fairfull-Smith, B. J. Morrow, V. Lussini, B. Kim, M. V. Bondar, S. E. Bottle, K. D. Belfield, *J. Am. Chem. Soc.* **2012**, *134*, 4721 – 4730; d) H. C. Heo, K. H. Kim, H. J. Kim, S. H. Baik, H. Song, Y. S. Kim, J. Lee, I. Mook-jung, H. M. Kim, *Chem. Commun.* **2013**, *49*, 1303 – 1305.

[26] H. M. Kim, B. R. Cho, *Acc. Chem. Res.* **2009**, *42*, 863 – 872.

[27] S. K. Bae, C. H. Heo, D. J. Choi, D. Sen, E. H. Joe, B. R. Cho, H. M. Kim, *J. Am. Chem. Soc.* **2013**, *135*, 9915 – 9923.

[28] H. J. Kim, C. H. Heo, H. M. Kim, *J. Am. Chem. Soc.* **2013**, *135*, 17969 – 17977.

[29] H. N. Kim, E. H. Lee, Z. Xu, H. E. Kim, H. S. Lee, J. H. Lee, J. Yoon, *Biomaterials* **2012**, *33*, 2282 – 2288.

[30] Z. Xu, S. K. Kim, J. Yoon, *Chem. Soc. Rev.* **2010**, *39*, 1457 – 1466.

[31] a) M, Fujihara, M. Muroi, K. Tanamoto, T. Suzuki, H. Azuma, H. Ikeda, *Pharmacol. Ther.* **2003**, *100*, 171 – 194; b) K. Schroder, P. J. Hertzog, T. Ravasi, D. A. Hume, *J. Leukoc. Biol.* **200**4, 75, 163 – 189; c) D. M. Paulnock, K. P. Demick, S. P. Coller, *J. Leukocyte Biol.* **2000**, *67*, 677 – 682.

[32] I. Engelmann, S. Dormann, M. Saran, G. Bauer, *Redox Rep.* **2000**, *5*, 207 – 214.

[33] J. Y. Shih, A. Yuan, J. J. W. Chen, P. C. Yang, *J. Cancer Mol.* **2006**, *2*, 101 – 106.

[34] a) O. Goldmann, E. Medina, *Front. Immunol.* **2012**, *3*, 420; b) S. K. Das, C. S. Lim, S. Y. Yang, J. H. Han, B. R. Cho, *Chem. Commun.* **2012**, *48*, 8395 – 8397.

[35] a) M. Prinz, J. Priller, *Nat. Rev. Neurosci.* **2014**, *15*, 300 – 312; b) D. Ito, Y. Imai, K. Ohsawa, K. Nakajima, Y. Fukuuchi, S. Kohsaka, *Mol. Brain Res.* **1998**, *57*, 1 – 9.

Received: January 20, 2015
Published online: February 20, 2015

